Tanzania Journal of Science 50(2): 281-294, 2024
ISSN 0856-1761, e-ISSN 2507-7961

In-situ investigation of Kinetics of Phase Transformation of Ti54M Titanium Alloy by Electrical Resistivity

Richard J Katemi
University of Dar es Salaam, School of Mines and Geosciences, Department of Mining and Mineral Processing Engineering, P. O. Box 35052, Dar es Salaam, Tanzania
Received 23 Dec 2023, Revised 13 Feb 2024, Accepted, Published June 2024
rkatemi@gmail.com
https://dx.doi.org/10.4314/tjs.v50i2.9

Abstract

The kinetics of phase transformation of Ti54M titanium alloy was investigated using electrical resistivity measurement for different heating cycles. The resulting microstructure parameters were analyzed using Aphelion software. It was found that α-phase starts to decompose to β-phase is between 600°C and 780°C. The temperature at which 100% β-phase was formed is 965°C. Beyond the temperature at which α-phase starts to decompose and despite the high heating rate of 10 °C/s, a rapid decrease of electrical resistivity which is attributed to dissolution of α-phase was observed. During isothermal holding, equilibrium was reached in about 15 minutes regardless of the holding temperature and differences in electrical resistivity observed at room temperature. A rapid increase in electrical resistivity during quenching which is attributed to martensitic transformation was observed and enhanced with increasing holding temperature. As expected, the fraction of α-phase, the surface density and average equivalent diameter of α-nodules decreased with increasing holding temperature. A good correlation between the variation of electrical resistivity and the fraction of α-phase obtained by image analysis after isothermal holding at different temperatures confirms that in-situ measurement of electrical resistivity can be used to determine the kinetics of phase transformation.

Keywords: Ti54M; Thermal loading; Electrical resistivity; Image analysis; Dissolution kinetics

Introduction

Despite high price due to high production cost, titanium alloys are widely used in aerospace industries due to their excellent combination of corrosion resistance, low density and high temperature strength properties (Markovsky and Semiatin 2010). For example, modern aeroengines components consisting of Titanium alloys can represent up to 30% by weight, which makes them second most used materials after Nickel superalloys components (Peters et al. 2005).

The improved mechanical properties of titanium alloys under thermal loading highly depend on the stability of microstructure characteristics such as phase composition, grain size and distribution, morphology and shape (Seshacharyulu and Dutta 2002). As a result, in situ investigation of kinetics of phase transformation during heat treatment cycles and the resulting microstructural characteristics have received due attention (Malinov et al. 2002). Several methods, such as high energy synchrotron x-ray diffraction (Barriobero-Vila et al. 2015), dilatometry (Chen et al. 2016), differential scanning calorimetry (Contrepois et al. 2011), and electrical resistivity (Hájek et al. 2007, Singh 2013), have been reported to study in-situ phase transformation kinetics. However, the electrical resistivity technique is a mature and well-known experiment technique (Hájek et al. 2007) and has found wide application in the investigation of kinetics of phase

transformation (Matsumoto 2004). In this technique, the component under investigation forms part of an electrical circuit and as the resistivity is the function of crystalline structure, the transformation kinetics can be obtained by monitoring how the resistance changes with temperature (Urbina et al. 2012). As a result, electrical resistivity has been proven to be a suitable technique to evaluate transformation kinetics in Ti-alloys although correlation with other techniques such as metallographic analysis remain necessary for a quantitative analysis of absolute phase fraction (Rodrigues et al. 2020). Although it is well known that Ti6Al4V is the most common titanium alloy and which accounts for more than 50% of the titanium alloy production, Ti54M is a titanium alloy that has a potential to reach even better mechanical properties than Ti6Al4V (Armendia et al. 2010). Previous research works on Ti54M alloy have mainly focused on the comparison of machinability both in different heat treatment conditions and different Ti-alloys such as Ti6A14V alloy (Khanna and Sangwan 2012, Rahim and Sharif 2006) and there is no comprehensive knowledge on the kinetics of phase transformations and the resulting microstructural characteristics of Ti54M titanium alloy.

This work investigated the kinetics of phase transformation of Ti54M titanium alloy using electrical resistivity and quantified the microstructural parameters after isothermal holding at different temperatures. Different algorithms using *Aphelion Dev* software were developed to quantify the different microstructural parameters. The parameters evaluated include: phase composition, average equivalent diameter (a.e.d) of α-nodules, nodule density, and nodules morphology. In addition, the kinetics of phase transformation was further confirmed using ThermoCalc software.

Material and Methods

Material

Ti54M titanium alloy with the chemical composition given in Table 1 was used for this investigation. A total of ten samples with a length of 40 mm and a diameter of 4 mm machined from a 200 mm diameter ingot treated in the α + β domain were used. Eight samples for electrical resistivity measurement, one sample for acquisition of initial microstructure and one sample for analysis of chemical composition. The initial microstructure consisted of α-phase (*both α-nodules and α-lamellae in grey*) and β-phase (*white*) as given in Figure 1. Analysis of the microstructure in this figure revealed 18% β-phase while the average equivalent diameter of α-nodules ranged from 9 to 11 µm.

Table 1: Chemical composition of the as-received sample

Element	**Mo**	**Fe**	**V**	**Al**	**C**	**O**	**Ti**
Mass-%	0.705	0.49	3.97	5.085	0.0204	0.158	Bal

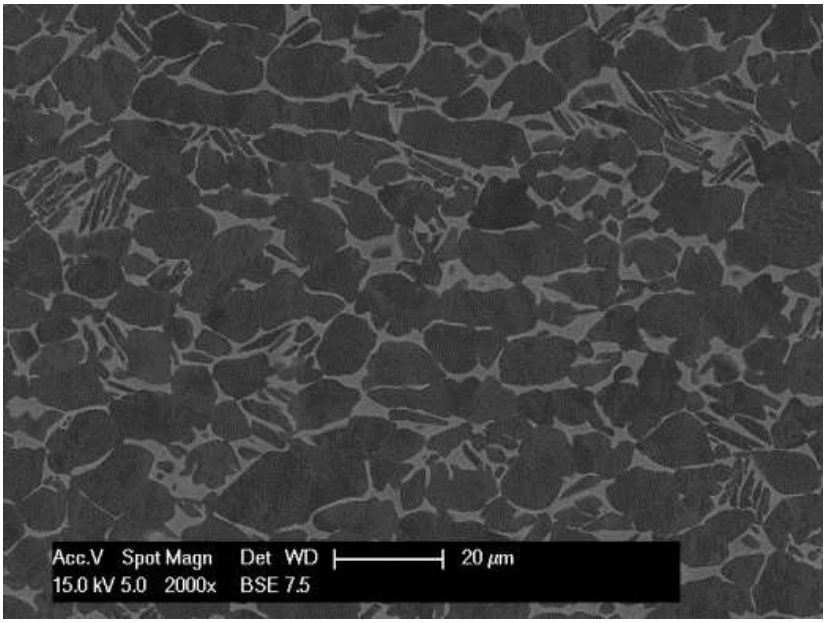

Figure 1: Initial microstructure of the as-received sample (*white: β-phase and grey: α-phase)*

Heat treatment and measurement of electrical resistivity

The heat treatments were carried out using a dilatometer with a continuous acquisition of dimensional behavior and resistivity evolution every 0.1 second for the whole heating cycle. The in-situ resistivity technique used was developed to study the behavior of metal alloys during thermal or thermomechanical treatments. In the current work the measurement technique was based on "four points" method (Archambault and Godard 2000). The “four points” method has proven to be a convenient tool for the resistivity measurement of small size (of the order of mm) samples (Singh 2013). The sample dimensions considered for measurement were diameter of 4 mm and length (ΔL) of 30 mm as illustrated in Figure 2. Four platinum wires for the passage of a constant direct current (2A) and for the measurement of the corresponding potential difference were welded on the surface of the sample. The sample was placed within an oven of a dilatometry device to carry out imposed heat cycles which were controlled in real time using an S-type thermocouple welded to the sample.

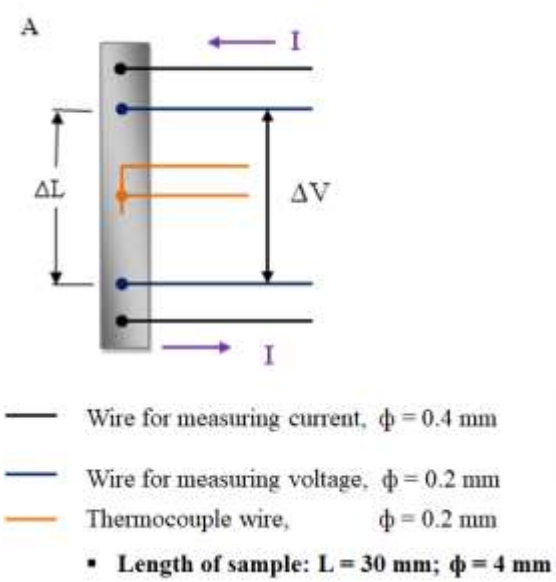

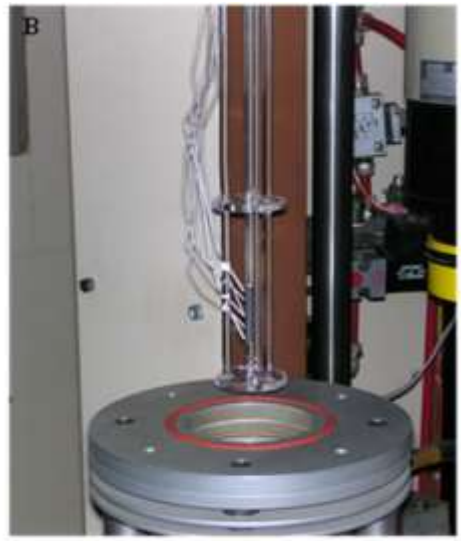

Figure 2: A) Sketch of the sample indicating principles of a "four-points" method and -B) experiment set-up for dilatometry experiment

In the first place, in-situ investigation was carried out to establish the transus temperature (T_β), the temperature at which 100% β-phase for Ti54M forms. Slow heating rate of 2 °C/min was used enabling to be as close to thermodynamic equilibrium conditions as possible. The T_β determined was 965°C. After the determination of T_β, heat treatment experiments were carried out at different pre-determined time-temperature cycles as shown in Figure 3. In each treatment, the heating cycle comprised of heating at a rate of 10°C/min from room temperature (T_R) to 400°C enabling to be close to thermodynamic equilibrium conditions and reduce chemical heterogeneity, isothermally holding at this temperature for 1 hour in order to desorb oxygen gas from the furnace and the sample leading to reduced susceptibility to surface and subsurface oxidation, heating at the same rate to the holding temperature, isothermally holding at this temperature for 1 hour, and finally quenching at helium gas down to 300°C followed by air cooling to room temperature. The holding temperatures were 840°C, 890°C, and 940°C. For each heating cycle, two experiments were conducted and the results were averaged; the results were reproducible. In order to avoid specimen oxidation, the experiments were carried out in a protective chamber with constant purging of helium gas.

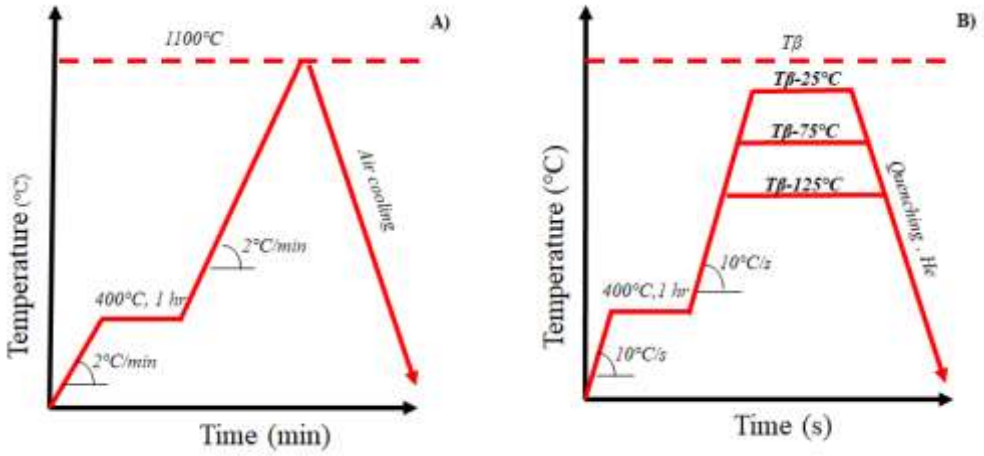

Figure 3: Sketch of heat treatment cycles: a) determination of transus temperature and -b) isothermal holding at different temperatures

Image acquisition

The images before and after heat treatment of the samples were acquired using Scanning Electron Microscope (SEM) - Philips XL30 SFEG in backscattered electron mode and electron acceleration voltage of 15 kV. The samples, polished using oxide polishing suspension (OPS) sheets, were observed without chemical attack. The α-phase is clearly differentiated from β-phase due to brighter contrast arising from high atomic number of elements in the β-phase. It has to be noted that image size was about 100 µm by 130 µm while the available mirror surface area of the sample for image acquisition was about 40,000 µm by 4000 µm. In order to obtain good counting statistics, 20 images per sample were taken from different points of the polished mirror surface of the sample.

Image analysis

Different algorithms using *Aphelion Dev* software were developed to quantify fraction of α-nodules, α-lamellae, grain size and distribution of α-nodules, surface density of α-nodules and form factor. These parameters were extracted after thresholding of the initial SEM image in Figure 4a. First, after thresholding, the contours of α-nodules were extracted. To do this, the software feature of creating skeleton by zone of influence of objects was used. During this stage, the α-lamellae phase was temporarily removed by performing erosion using a structuring element of square shape followed by reconstruction. The image obtained at the end of these operations is shown in Figure 4b. The parameter extracted from this image is the fraction of α-nodule phase. The surface density, average equivalent diameter, and the form factor (g*iven as the ratio of diameters of the minimum and maximum ferrets of α-nodules*) were determined after removing the α-nodules in contact with the edge of the image as illustrated in Figure 4c. Finally, the fraction of α-lamellae phase was obtained using logical operators which keep only the α-lamellae phase as shown in Figure 4d.

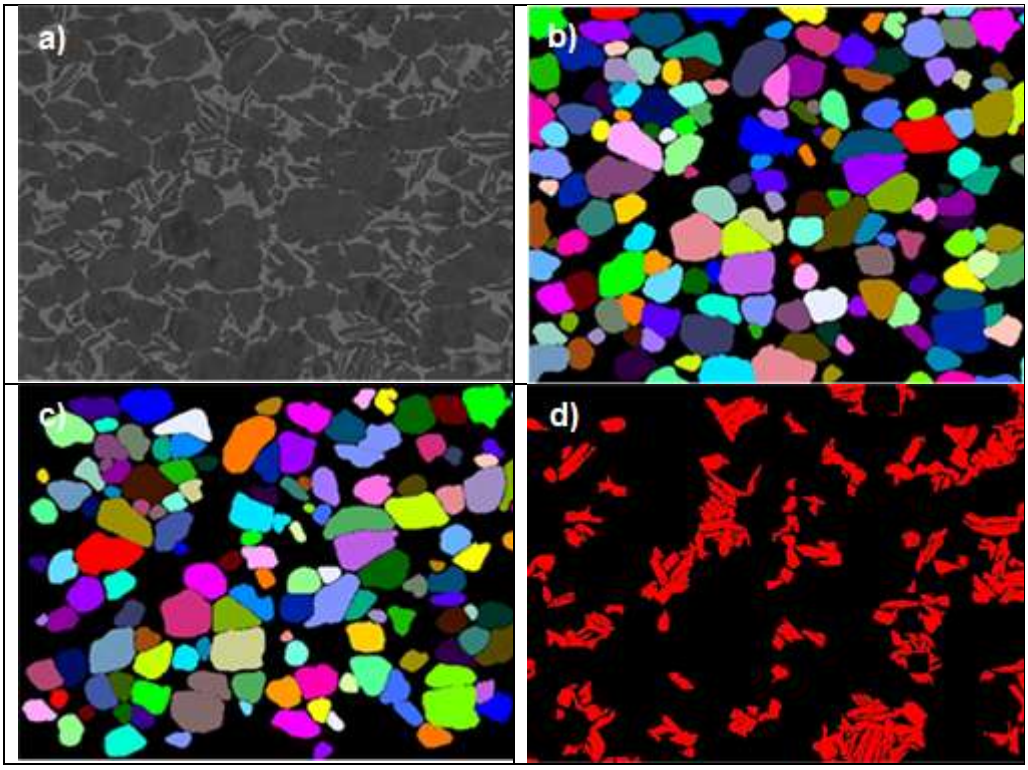

Figure 4: Image analysis after isothermal holding: (a) initial SEM image, (b) determining of α-nodules phase fraction, (c) determination of density and size distribution of α-nodules, and (d) determination of α-lamellae phase fraction

Results and Discussion

Electrical resistivity

The determination of transus β, the temperature at which 100% of β-phase is formed, was carried out by imposing slow heating of 2 °C/min. The transus β measurement was doubled and the results were reproducible. Figure 5 presents the evolution of electrical resistivity during heating from room temperature to 1100ºC. On heating from room to about 400ºC is linked to increase in temperature while between 400 and 600ºC is mainly due to changes in chemical composition in the two phases. It has to be noted that before heat treatment the initial microstructure of the samples was characterized by the presence of phase α + β. A pronounced decrease in electrical resistivity between 600°C and the transus temperature (Tβ = 965ºC). This strong decrease is clearly attributed to the dissolution of the α-phase. Beyond Tβ, the electrical resistivity changes little because the sample is in the single-phase domain β.

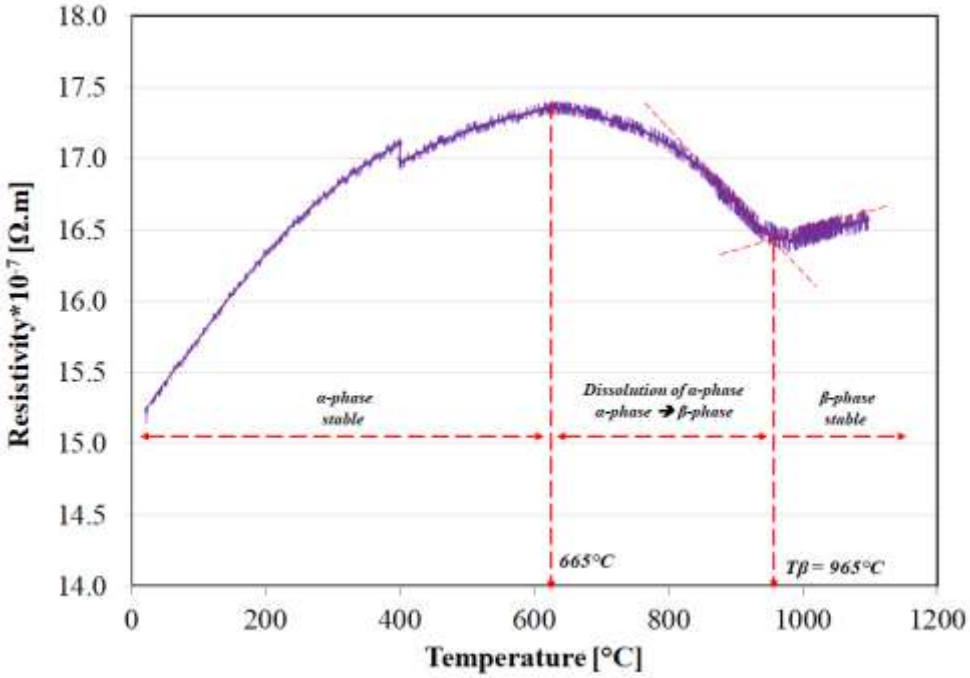

Figure 5: Determination of transus temperature (Tβ) for Ti54M

Figure 6 presents the changes in electrical resistivity during heating, isothermal holding and quenching stages. In general, electrical resistivity is sensitive to temperature and microstructural changes. As seen from Figure 6a, the discrepancies of electrical resistivity values at room temperature can be attributed to structural heterogeneity and inhomogeneous chemical compositions as the samples were extracted from different points of as-received ingot with diameter of 200 mm. From room temperature to about 400°C, the electrical resistivity increases substantially linearly with temperature behaving like a pure metal in which the influence of impurities is negligible (McQuillan 1956). From 400°C to the temperature at which α-phase starts to dissolve (α ==> β), a relative decrease of change of electrical resistivity with temperature can be observed. The temperature at which α ==> β during heating was about 757°C for the sample held at 840°C, 780°C for the sample held at 890°C, and 613°C for the sample held at 940°C. The relative decrease in this range is attributed to the presence of impurities mainly oxygen of which titanium has high chemical affinity to it. Despite the high heating rate of 10°C/s, between 613°C and 780°C, a decrease of electrical resistivity with temperature which is attributed to dissolution of α-phase into β-phase can be observed.

The changes of electrical resistivity with time during the different isothermal holding at 840°C, 890°C, and 940°C are given in Figure 6b. At all holding temperatures, the change in electrical resistivity with time is relatively low and this signify that large proportion of α-phase has dissolved during the heating stage. At each condition, equilibrium is reached very quickly despite the differences in electrical resistivity observed at room temperature. The equilibrium condition is reached in about 15 minutes regardless of the holding temperature as no further dissolution of α-phase occurs and homogeneous chemical composition.

Figure 6c shows the variation of electrical resistivity as a function of temperature during the cooling from the isothermal holding temperatures. A rapid increase in electrical resistivity during quenching is observed which is enhanced with increasing holding

temperature. The increase in electrical resistivity is due to exothermic martensitic transformation (β→α') which is accompanied by release of heat (Liu 2009). Further, a strong exothermic reaction during quenching is observed at the point a peak in electrical resistivity is observed as illustrated Figure 7 which shows variation of temperature with time during quenching. As seen in Figure 7, a slight discontinuity in temperature which is attributed to exothermic martensitic transformation can be observed. In this case, the exothermic martensitic transformation starts at about 410°C, 640°C, and 680°C for the specimen held at 840°C, 890°C, and 940°C respectively. The location of slight increase in temperature is in good agreement to the temperature at which the rapid increase on electrical resistivity during cooling is observed.

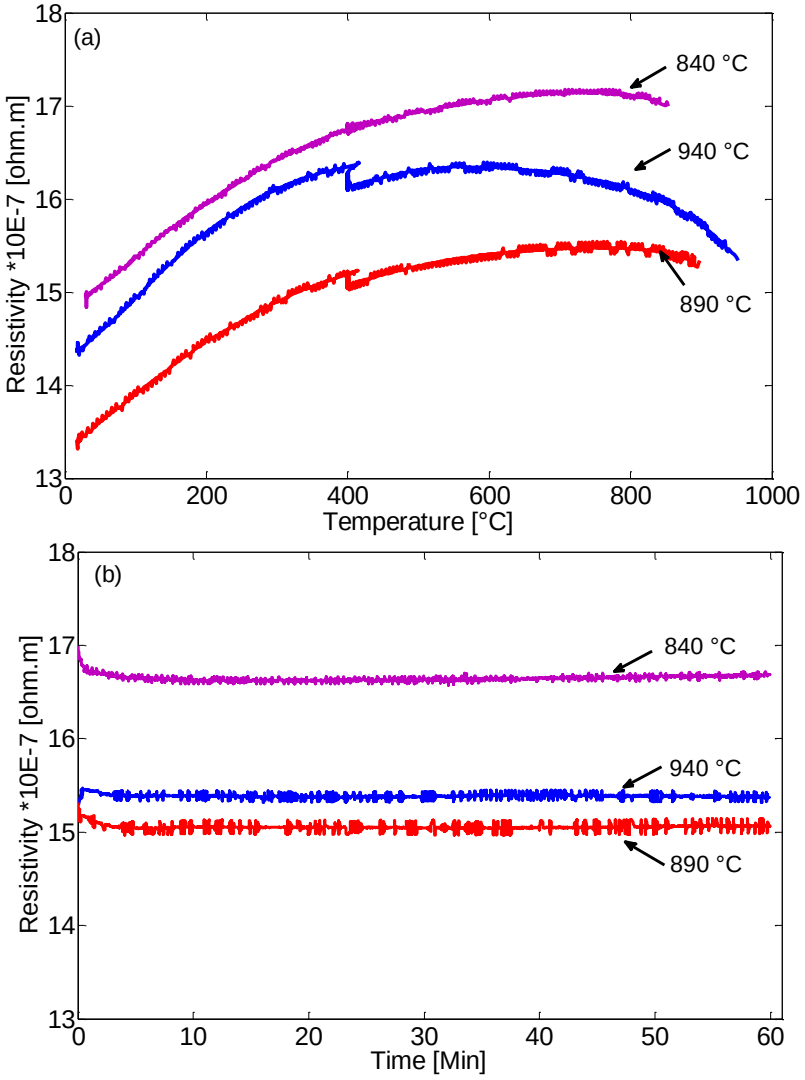

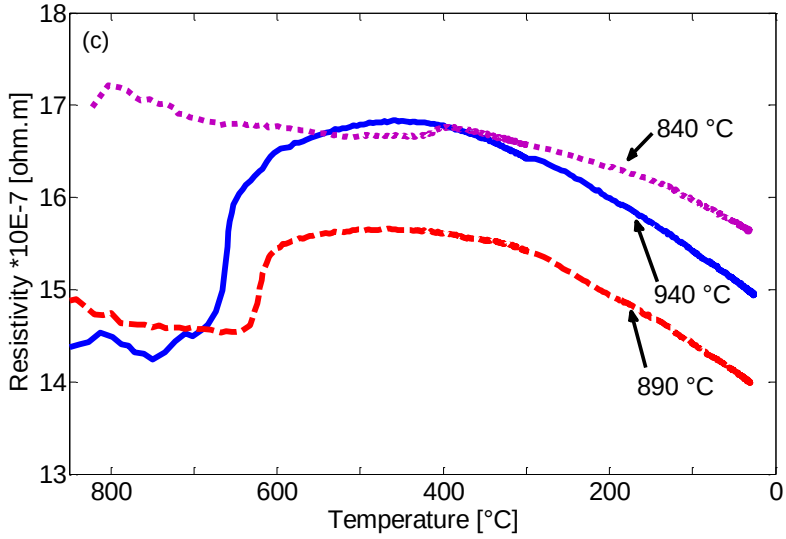

Figure 6: Evolution of electrical resistivity during heat treatment cycle: a) heating, b) isothermal holding, c) quenching.

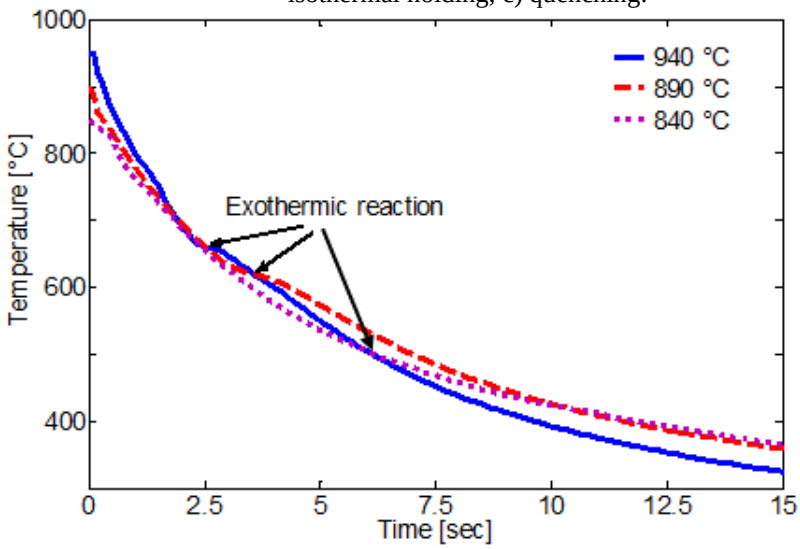

Figure 7: Variation of temperature with time during quenching.

Microstructures and image analysis

Figure 8 presents the microstructures before and after heat treatment of the Ti54M alloy. The as-received state (Figure 8a) is characterized by duplex microstructure with α-phase (majority) in gray surrounded β-phase (minority) in white. The α-phase exists in both nodules as well as in lamellar form in the matrix of β-phase. It has to be noted that specimens were not chemically attacked; α-phase can be differentiated from β-phase due to brighter contrast arising from atomic number elements in the β-phase. The initial α-phase composition of the as-received sample (Figure 8a) was 82 % with initial nodules average equivalent diameter of 7.75 µm and nodule density of 11.4 $*10^{-3}/\mu m^{-2}$.

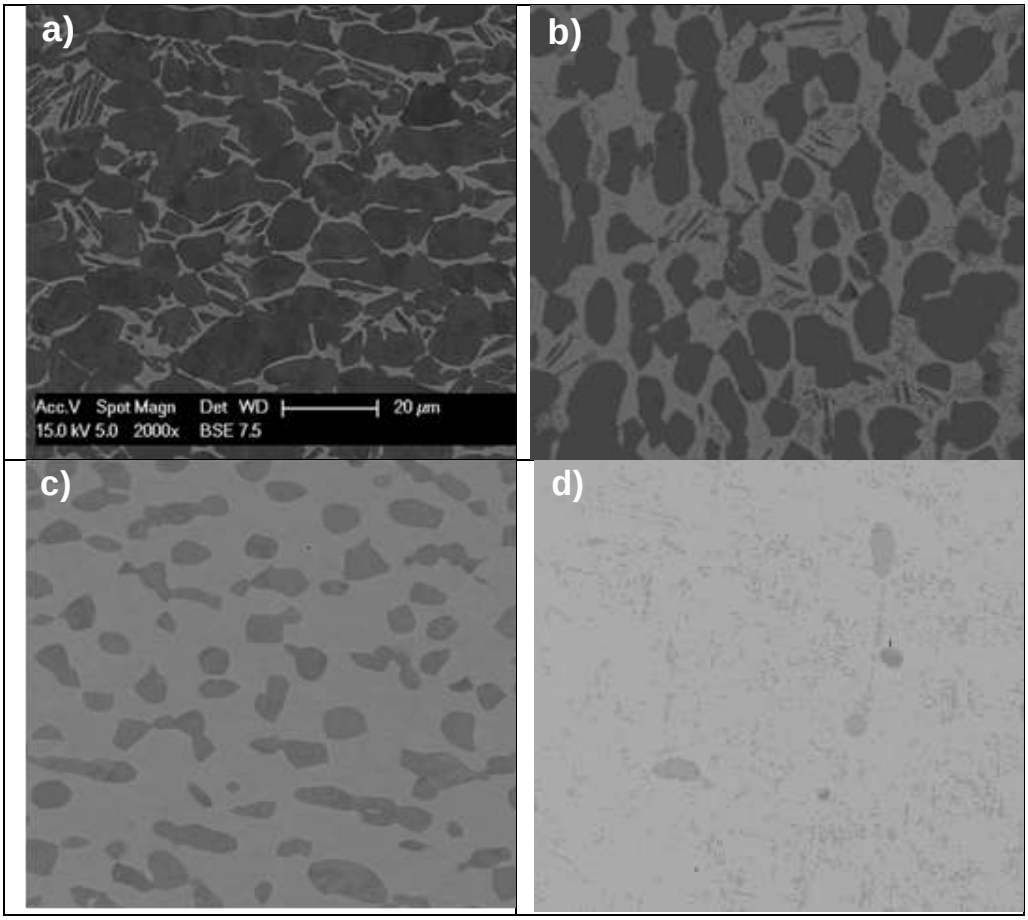

Figure 8: Typical microstructures of Ti54M alloy for as-received and after isothermal holding for 1 hour and subsequent quenching: a) as-received, b) 840°C, c) 890°C, d) 940°C

Figures 8b and -8c show the microstructures in the transversal direction obtained after isothermal holding at 840°C, 890°C and 940°C for 1 hour followed by quenching at helium. The microstructures (α-nodules) are highly dependent on the holding temperature. The α-phase exists only in nodule form except the sample held at 840°C (Figure 8b) which exists in nodule as well as in lamellar form. As it is evident from Figure 8d, very few α-nodules remain after isothermally holding at 940°C the temperature which is close to the transus temperature (965°C) for Ti54M titanium alloy.

Image analysis to quantify phase composition (α-nodule and lamellar), surface density, average equivalent diameter (a.e.d) and form factor of α-nodules, the parameters which are responsible for reduction of flow stress during forging was done using different algorithms *Aphelion software* algorithms. The results are presented in Table 2. As expected, the fraction of α-phase (nodule + lamellar), nodule density and the a.e.d of α-nodules decrease when the holding temperature increase. The phase composition (α-phase) obtained after analysis of 20 images for each holding temperature were 37, 21.3 and 1.5 mass. -% of α-phase (nodule) sample held isothermally at 840°C, 890°C, and 940°C, respectively. On the other hand, no particular tendency is observed for the form factor. As can be seen from the Table 2, α-lamellae have higher dissolution kinetics in comparison to α-nodules. For example, from room temperature to 840°C about 50

mass-% of α-lamellae dissolved whereas only 31 mass-% of α-nodule dissolved in the same temperature range. The high dissolution kinetics of α-phase at high temperatures (>840 °C) indicates that α-phase in Ti54M alloy is highly unstable and its mechanical properties can be considerably affected by the decrease in fraction of α-phase, a.e.d and morphologies of α-nodules. In view of reduction of flow stress during processing, the current trend, however, is toward formation of ultra-fine grains refinement and their stability at high temperatures in which hydrogenation treatment has been widely used as the grain refinement technique (Guitar 2009). Increase of tensile stress as well as reduction of flow stress with degree of grain refinement has been reported by Yoshimura and Nakahigashi (Yoshimura and Nakahigashi 2002).

Following components quantified above, the normal distribution of α-nodules after isothermal holding at different temperatures was established and given in Figure 9. In order to avoid overloading the figure, only the as-received, isothermal holding at Tß-75°C and Tß-25°C were considered. It can be observed from this figure that the α-nodule size distribution shifts towards the small size and the disparity between the α-nodules decreases as the holding temperature increases mainly due to diffusional phase transformation process of α phase to β-phase during heating stage.

Table 2: Quantitative data obtained by image analysis after isothermal holding at different temperatures.

State	Fraction of α-nodules (%)	Fraction of α-lamellae (%)	Density of α-nodules (#.10^{-3}/µm^{-2})	a.e.d of α-nodules (µm)	Nodule form factor
As-received	54	28	11.4	7.8	0.68
Tβ-125°C	37	14	9.6	7.0	0.70
Tβ-75 °C	21.3	0	8.6	5.6	0.58
Tβ-25°C	1.5	0	0.85	4.7	0.71

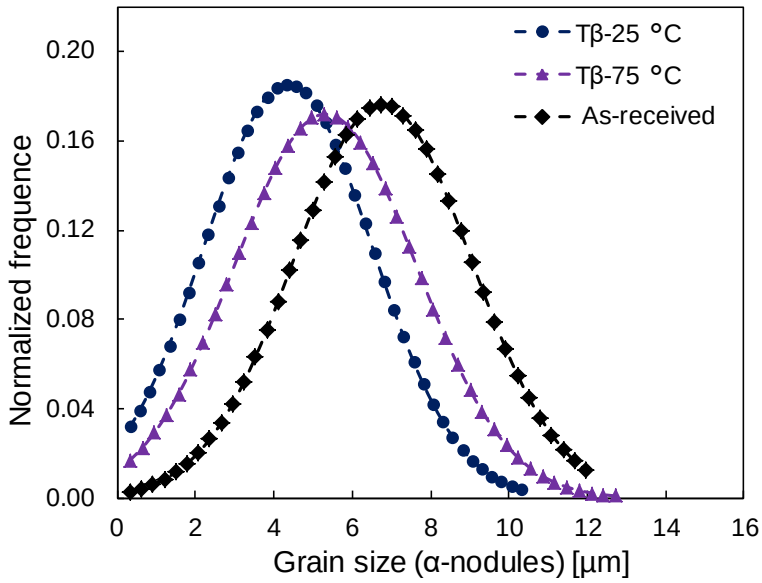

Figure 9: Distributions of α-nodule grain size for different holding temperatures

Comparison of variation of electrical resistivity as a function of temperature against

the total fraction of α-phase at different holding temperatures (by image analysis) and ThermoCalc® calculation is given in Figure 10. The ThermoCalc calculation was done using the chemical composition provided in Table 3. The content of oxygen was adjusted to reach Tβ of 975°C. It is observed that at all temperatures the experimental fraction α-phase is lower than that determined using ThermoCalc calculation. The higher content of α-phase determined using ThermoCalc is attributed to the difference in chemical composition in the samples and the ones used during ThermoCalc calculations. In contrast, the decrease of fraction of α-phase (*estimated by image analysis*) with increasing holding temperature correlates well with the decrease of electrical resistivity with temperature. The good correlation confirms that in-situ measurement of electrical resistivity can be used to determine the kinetics of phase transformation.

Table 3: Chemical compositions used during ThermoCalc calculation.

Element	Al	V	Fe	Mo	O	Ti
wt%	5.08	3.97	0.49	0.70	0.35	Bal

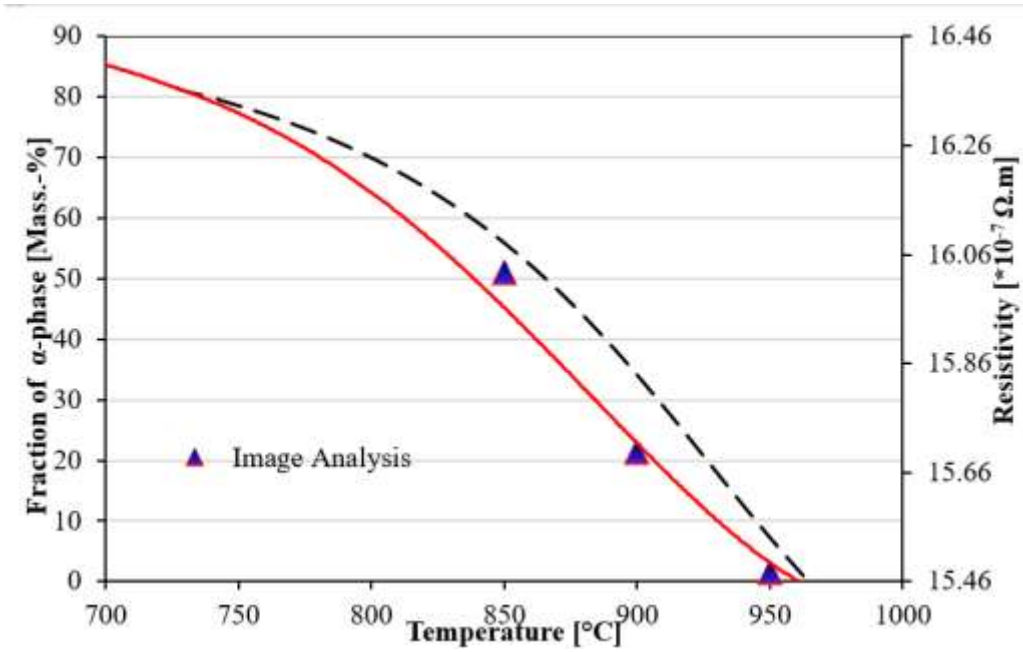

Figure 10: Variation of fraction of α-phase and resistivity as a function of temperature.

Conclusion

This work investigated the kinetics of phase transformation of Ti54M titanium alloy using in situ measurement of electrical resistivity for different heating cycles. The resulting microstructures after isothermal holding at different temperatures were analyzed using Aphelion software algorithms. From this investigation, the transus temperature established for Ti54M was 965°C. During the heating stage, a discrepancy in electrical resistivity at room temperature is observed which is attributed to structural heterogeneity and inhomogeneous in chemical compositions. Despite of the high heating rate of 10 °C/s, beyond 600°C, a rapid

decrease of electrical resistivity is observed which marks the beginning of α-phase dissolution. During isothermal holding, equilibrium condition is reached in about 15 minutes regardless of the holding temperature. Furthermore, a rapid increase in electrical resistivity during quenching which is enhanced with the increase in holding temperature is observed.

As expected, the fraction of α-phase (nodule + lamellar), the density of α-nodules and the average equivalent diameter of α-nodules decrease when the holding temperature increase. A good correlation between the evolution of electrical resistivity and the fraction of α-phase obtained by image analysis after isothermal holding at different temperatures confirms that in-situ measurement of electrical resistivity can be used to determine the kinetics of phase transformation.

References

Archambault P and Godard D 2000 High temperature precipitation kinetics and TTT curve of a 7xxx alloy by in-situ electrical resistivity measurements and differential calorimetry. *Scr. Mater*. 42(7): 675–680.

Armendia M, Garay A, Iriarte LM and Arrazola PJ 2010 Comparison of the machinability of Ti6Al4V and TIMETAL®54M using uncoated WC-Co tools. *J. Mater. Process. Technol.* 210(2): 197-203.

Barriobera-Vela P, Requena G, Shwarz S, Warchomicka F and Buslaps T 2015 Influence of phase transformation kinetics on the formation of α in a β-phase quenched Ti5Al5Mo3Cr1Zr alloy. *Acta Mater*. 95: 90-101.

Chen F, Xu G, Zhang X and Zhou K 2016 Exploring the phase transformation in β-quenched Ti-55531 alloy during continuous heating via dilatometric measurement, microstructure characterization, and diffusion analysis. *Metall. Mater. Trans. A*. 47: 5383-5394

Contrepois Q, Carton M and Lecomte-Beckers J 2011 Characterization of the β-phase decomposition in Ti-5Al-5Mo-5V-3Cr at slow heating rates. *Open J. Met*. 1: 1-11.

Guitar A, Vigna G, and Luppo MI 2009 Microstructure and tensile properties after thermohydrogen processing of Ti-6Al-4V. *J. Mech. Behav. Biomed. Mater*. 2: 156-163.

Hájek M, Veselý J and Cieslar M 2007 Precision of electrical resistivity measurements. *Mater. Sci. Eng. A* 462: 339-342.

Khanna N and Sangwan KS 2012 Comparative machinability study on Ti54M titanium alloy in different heat treatment conditions. *Proc IMechE, Part B: J Eng Manuf*. 227(1): 96-101.

LIU Y 2009 Thermodynamics of the shape memory effect in Ti-Ni alloys. In: Yoneyama T and Miyazaki S (Eds) *Shape memory alloys for Biomedical Applications* (pp. 37–68), Woodhead Publishing Limited, England.

Malinov S, Markovsky P and Sha W 2002 Resistivity study and computer modelling of the isothermal transformation kinetics of Ti-8Al-1Mo-1V alloy. *J. Alloy. Compd*. 333(1-2): 122-132.

Markovsky PE and Semiatin SL 2010 Microstructure and mechanical properties of commercial-purity titanium after rapid (induction) heat treatment. *J. Mater. Process. Technol*. 210(3): 518-528.

Matsumoto H 2004 Irreversibility in transformation behavior of equiatomic nickel-titanium alloy by electrical resistivity measurement. *J. Alloys. Comp*. 368(1-2): 182-186.

McQuillan AD and McQuillan MK 1956 Titanium. In: Finniston HM (Ed) *Metallurgy of the rarer metals* vol. 4, Butterworths Scientific, London.

Peters M, Hemptenmacher J, Kumpfert J and Leyens C 2003 Structure and Properties of Titanium and Titanium Alloys. In: Leyens C and Peters M (Eds) *Titanium and Titanium Alloys: Fundamentals and Applications*, (pp. 1-36), Wiley-VCH Verlag GmbH, Weinheim.

Rahim EA and Sharif S 2006 Investigation on tool life and surface integrity when drilling Ti-6Al-4V and Ti-5Al-4VMo/Fe. *JSME Int. J. Series C*. 49920: 340-345.

Rodrigues MCM, Garcin T and Militzer M 2020 In-situ measurement of the β to α phase transformation kinetics in a Ti-5553alloy using laser ultrasonics. MATEC Web of Conferences 321, 12013. The 14th World Conference on Titanium

Seshacharyulu T and Dutta B 2002 Influence of prior deformation rate on the mechanism of β →α+β transformation in Ti-6Al-4V. *Scr. Mater*. 46(9): 673-678.

Singh Y 2013 Electrical resistivity measurements: A review. *Int. J. Mod. Phys. Conf. Ser*. 22: 745-756.

Urbina C, De la Flor S, Gispert-Guirado F and Ferrando F 2012 New interpretation of the electrical resistivity measurements for obtaining NiTi SMA stress-free transformation temperatures. In *Proc. ASME 11th Biennial Conf. Eng. Syst. Design Anal.*, Nantes, France.

Yoshimura H and Nakahigashi J 2002 Ultra-fine-grain refinement and superplasticity of titanium alloys obtained through protium treatment. *Int. J. Hydrog. Energy*. 27(7-8): 769-774.